Title

Cortical projection to the subventricular zone and its effect on adult neurogenesis in mice

Author names and affiliation

Rei Ota[1], Ryota Yoshida[1], and Tetsuji Mori[1]

[1]Department of Biological Regulation, School of Health Science, Faculty of Medicine, Tottori University, Yonago, Japan

Email addresses

Rei Ota: m21m5007x@edu.tottori-u.ac.jp

Ryota Yoshida: m22m5034y@edu.tottori-u.ac.jp

Tetsuji Mori: mori-te@tottori-u.ac.jp

Corresponding author

Tetsuji Mori

Department of Biological Regulation, School of Health Science, Faculty of Medicine, Tottori University, 86 Nishi-Cho, Yonago 683-8503, Tottori, Japan.

E-mail: mori-te@tottori-u.ac.jp

Conflicts of interest

There is no conflict of interest.

Highlights

The cerebral cortex projects axons to the subventricular zone in adult mice.

Corticostriatal axons are in contact with neuroblasts in the subventricular zone.

Interruption of cortical projection dispersed the migration pathway of neuroblasts.

Abstract

Various brain regions/nuclei project axons to the subventricular zone (SVZ), a postnatal neurogenic niche. In adults, neurogenesis is controlled by neuronal activity, via neurotransmitters. Glutamate is a major excitatory neurotransmitter, and glutamate receptors are expressed in SVZ cells. Although the cerebral cortex is a major source of glutamate and the medial cortex projects axons to the medial striatum next to the SVZ, it remains unclear whether cortical neurons regulate adult neurogenesis *in vivo*. First, to analyze axonal projection, plasmid vector expressing DsRed was introduced to the medial cortex by *in utero* electroporation. At the adult stage, DsRed-labeled axons were detected in the dorsolateral, striatal, and septal areas of the SVZ, and where they were in contact with neuroblasts. Furthermore, maturation of the cortical projection and the SVZ appeared to synchronize during postnatal stages. Next, stab injuries were made in the bilateral medial cortex to interrupt cortical input to the SVZ. At 17 days post-injury, cell proliferation in the SVZ and tangential migration of neuroblasts to the olfactory bulb were not significantly affected. There were clusters of neuroblasts in the striatum close to the SVZ in all experimental groups, but the number and size of neuroblast clusters were significantly larger in the medial cortex-injured group compared with the other experimental groups. These neuroblast clusters had a morphology of tangentially migrating cells to the olfactory bulb. These results suggest that cortical input to the SVZ inhibits the radial migration of neuroblasts to converge with the migration pathway *in vivo*.

Key words

Adult neurogenesis, cortical projection, cell migration, injury, subventricular zone

Funding

This work was supported by JSPS KAKENHI, Grant Number: JP21K06735.

1. Introduction

In mammals, there are two well-known neurogenic areas in the adult brain: the subventricular zone (SVZ), located around the lateral ventricles (LVs), and the hippocampal dentate gyrus [1]. In the adult SVZ, glial fibrillary acidic protein (GFAP)-expressing cells are neural stem cells (Type B cells), and they sequentially differentiate into transient amplifying cells (Type C cells) and proliferating neuroblasts (Type A cells). Type A cells express doublecortin (DCX) and tangentially migrate to the olfactory bulb (OB) through the rostral migratory stream (RMS). Finally, Type A cells radially migrate toward the outer layers of the OB [1].

Adult neurogenesis is tightly regulated by many factors, and neurotransmitters derived from various brain regions/nuclei affect diverse aspects of neurogenesis in the SVZ [1,2]. For example, ablation of the substantia nigra, a source of dopamine, results in reduced proliferation of SVZ cells [3]. Serotonin derived from the raphe nuclei enhances the proliferation of SVZ cells [4–6]. Phasic and tonic activation of GABA-A receptors have positive and negative effects, respectively, on the proliferation of SVZ cells [7,8], while the activation of GABA-A receptors attenuates the migration of Type A cells [8–10].

Glutamate is a major excitatory neurotransmitter. Glutamate receptors are classified into metabotropic and ionotropic receptors, and ionotropic receptors are further subdivided into N-methyl-D-aspartate (NMDA), α-amino-3-hydroxy-5-methyl-4-isoxazolepropionic acid (AMPA), and kainite (KA) receptors [11]. The effect of glutamate on adult neurogenesis is complex. Many experiments have been performed using cultivated SVZ cells; however, it must be kept in mind that cultivation changes the properties of neural stem/precursor cells [12]. To date, histological and electrophysiological experiments have confirmed that Type A cells express metabotropic glutamate receptors (mGluR4, mGluR5), NMDA receptors, AMPA receptors (GluR1, GluR2), and a KA receptor (GluK5) [13–17]. Administration of an mGluR4 agonist in the LVs inhibits proliferation and promotes neuronal differentiation of Type A cells [17]. On the other hand, mGluR5 knockout mice show a smaller number of proliferating cells in the SVZ [13]. Blocking NMDA receptors enhances apoptosis of Type A cells *in vivo* [15], but activation of AMPA receptors enhances the proliferation of Type A cells [16]. In a whole-mount SVZ culture system, application of a GluK5 antagonist increased the migration speed of Type A cells [14].

Platel et al. reported that astrocytes in the SVZ/RMS are a major source of the glutamate that regulates adult neurogenesis; these authors also suggested that neuronal glutamate could have a minor effect on adult neurogenesis [15]. However, a whole-mount culture system that they used is free from axonal projections from the cortex. The striatum receives abundant glutamatergic axons from the cerebral cortex. In particular, the medial cortex, including the prelimbic and cingulate cortex, projects axons to the most medial part of the striatum, close to the SVZ [18–20]. Recently, cortical glutamatergic input to the SVZ was suggested [16], but direct evidence of cortical projection to the SVZ and its effects on adult neurogenesis *in vivo* is lacking.

In the present study, we introduced DsRed-expressing plasmid vector into the medial cortex by *in utero*

electroporation, to visualize axons projecting to the striatum; we then analyzed the maturation of corticostriatal projections and the postnatal SVZ. Furthermore, by injuring the medial cortex, we examined the effects of the cortex on neurogenesis *in vivo*.

2. Materials and methods

2.1 Animals

Male and female ICR mice were used for the experiments. For the analysis of adult brains, six-week-old mice were used. For the analysis of embryonic brains, timed pregnant mice were used. The day when a vaginal plug was detected was defined as embryonic day 0 (E0). All experiments were performed in compliance with the Guidelines for Animal Experimentation of the Faculty of Medicine, Tottori University, under the International Guiding Principles for Biomedical Research Involving Animals.

2.2 *In utero* electroporation

A plasmid vector expressing DsRed, driven by the CAG promoter, was used. Pregnant female mice were anesthetized by the intraperitoneal (ip) injection of a mixture of medetomidine (0.3 mg/kg), midazolam (4 mg/kg), and butorphanol (5 mg/kg) in phosphate buffered saline (PBS) (MMB). Approximately 1 to 2 μl of endotoxin-free plasmid DNA (4 μg/μl) containing 0.01% of Fast Green in PBS was injected into one side of the LV of E13 or E14 embryos, using a pulled glass capillary. The embryos' heads were held with forceps-type electrodes (CUY 650P5, NEPA GENE, Chiba, Japan) thorough the uterine wall at an angle of about 45°. Square electric pulses were delivered (five pulses of 40 V for E13 embryos or 45 V for E14 embryos, with 50 msec durations at 950 msec intervals), using an electroporator (CUY21SC, NEPA GENE) [21].

2.3 Cortical stab injury

Adult male mice were anesthetized by the ip injection of MMB and fixed to a stereotaxic instrument. The cranial bone was drilled, and the bilateral medial cortex (Medial group, approximately 0.5-mm lateral from the midline and approximately 2 mm in the anteroposterior axis) or the bilateral primary motor/somatosensory cortex (Lateral group, approximately 2.5-mm lateral from the midline and approximately 2 mm in the anteroposterior axis) were manually stabbed with a needle. Care was taken over the depth of the injury to prevent disruption to the corpus callosum. In addition, a control group of mice without any surgery was prepared (Naive group). Mice were fixed at 4- or 17-days post-injury (DPI). For the 17 DPI group, BrdU (5-bromo-2′-deoxyuridine, 10 mg/ml in PBS) was ip injected at a dose of 50 mg/kg, 10 days after surgery. Age- and sex-matched mice were used in each experiment.

2.4 Tissue preparation

Mice older than postnatal day (P) 7 were euthanized with pentobarbital (200 mg/kg, ip) and transcardially perfused with 0.9% NaCl, followed by 4% paraformaldehyde/PBS (4% PFA). Neonatal mice were deeply anesthetized with hypothermia and perfused as described above. The brains were removed and postfixed with 4% PFA overnight. Fixed neonatal (~P7) brains and a pair of the adult OBs were immersed in 10% fish gelatin (Sigma, St. Louis, MO, USA)/PBS for 12 h at 10 °C, embedded in 10% gelatin/PBS, and fixed with 4% PFA overnight. Gelatin-embedded neonatal and older (P21 and adult) mouse brains were cut using a micro-slicer in 60-μm-thick free-floating coronal sections. Adult brains and gelatin-embedded adult OBs were cryoprotected with 20% sucrose in PBS, snap frozen on dry ice, and cut using a cryostat in 30-μm-thick free-floating coronal sections.

2.5 Antibodies and immunohistochemistry

The sections were incubated with primary antibodies diluted with 1% BSA/0.3% Triton X-100/PBS overnight at 4 °C, followed by secondary antibodies for 2 h at 4 °C. To detect cells that had incorporated BrdU, sections were pretreated with 2 M HCl for 30 min at 37 °C, followed by neutralization with 0.1 M sodium borate (pH 8.5) for 15 min, twice. To detect Ki67 immunopositive (+) cells, the sections were treated with HistoVT One (Nacalai Tesque, Kyoto, Japan) for 20 min at 70 °C for antigen retrieval. Antibodies used are listed in Table 1. Gelatin-embedded sections were attached to gelatin-coated glass slides and treated with TrueView Autofluorescence Quenching Kit (Vector, Newark, CA, USA). To visualize nuclei, sections were coverslipped with aqueous mounting medium containing 0.2% n-propyl gallate, 50% glycerol, 5 μg/ml Hoechst 33258, and PBS.

2.6 Image acquisition and processing

Images were acquired using an All-in-One epifluorescence microscope (BZ-X800, KEYENCE, Osaka, Japan). Single optical images were acquired using a confocal microscope (LSM 780, Carl Zeiss, Oberkochen, Germany) or the BZ-X800 with a sectioning function. For quantification of fluorescence intensity, black-and-white images with 16-bit depth were acquired using BZ-X800. Exposure time was adjusted to cover all the fluorescence intensities within the dynamic range of the digital camera. The images were acquired using the same exposure time to compare the fluorescence intensities between each experimental condition.

2.7 Quantification and statistical analysis

To quantify Ki67(+) and DCX(+) cells in the SVZ, every tenth coronal section was collected from 0.74 to 0.02 mm anteroposterior to the bregma, and four sections were analyzed from each mouse. To quantify BrdU(+) cells in the adult OBs, three randomly selected sections collected from 4.28- to 3.56-mm anteroposterior to the bregma were analyzed from each mouse. The number of DCX(+) cells was manually quantified under an epifluorescence microscope. For quantification of Ki67(+) and BrdU(+) cells, tiled single optical layer images were acquired using a BZ-X800 equipped with a sectioning function. Then, images were analyzed with ImageJ software (https://imagej.nih.gov/ij/), using the

particle analysis function. The mean fluorescence intensity of Iba1 immunostaining in the medial halves of the striatum was measured using Image J software. Statistical analysis was performed using EZR (ver. 1.56), a free statistical software package [22]. The level of significance between three experimental groups was determined using a one-way ANOVA followed by Tukey's *post hoc* test (a parametric analysis) or the Kruskal–Wallis test followed by the Steel–Dwass test (a non-parametric analysis), depending on the results of the Shapiro–Wilk normality test and Bartlett's test for homogeneity of variances. Statistical significance was set at $p < 0.05$. Six mice in each condition were analyzed.

3. Results

3.1 Axonal projection from the medial cortex to the SVZ

First, axonal projection from the medial cortex to the SVZ was analyzed. The corticostriatal projection neurons are born between E12 and E14, with a peak at E13; these neurons project axons to the bilateral striatum, contralateral cingulate cortex, and septum [23,24]. Thus, DsRed-expressing plasmid vector was unilaterally introduced to the medial cortex by *in utero* electroporation (Supplemental Fig. 1). At P21, DsRed-labeled axons invaded from the dorsolateral area of the SVZ, where the largest number of neural stem/precursor cells was present (Fig. 1A and Supplemental Fig.2A2 and 2A3). The greatest abundance of DsRed-labeled axons was detected in the ipsilateral medial striatum (Supplemental Fig. 2A4 and 2A5). Some DsRed-labeled axons were detected in the septal and the striatal areas of the SVZ (Fig. 1B and 1C). DsRed-labeled axons in the SVZ were in contact with DCX(+) cells (Fig. 1 and Supplemental Fig. 3, arrows).

Next, the development of the axonal projections was analyzed. The DsRed-labeled axons began to enter the ipsilateral and contralateral striatum from the dorsolateral areas of the SVZs at around the time of birth (data not shown). During the early neonatal stages, the DsRed-labeled axons were diffusely distributed from the medial to the lateral striatum (Fig. 2A-2C), but they gradually localized at the medial striatum. Finally, at P21, DsRed-labeled axons were densely packed in the most medial part of the striatum (Fig. 2D-2F). The germinal layers around the ventricular wall became dramatically thin in the first postnatal week and continued to mature until P21 (Fig. 2A' and 2D'). The anti-GFAP antibody labeled radial glia at the neonatal stages, and a final GFAP-immunostaining pattern was established at around P21 (Fig. 2B, 2C, 2E, and 2F). These results suggest that maturation of axonal projections from the medial cortex correlates with maturation of the postnatal SVZ and that cortical input has some effect on adult neurogenesis.

3.2 Effects of medial cortical injury on adult neurogenesis

To investigate the role of cortical input in adult neurogenesis, bilateral stab injuries to the medial cortex were made in the brains of adult mice (Medial group). It is known that SVZ cells are activated by

various types of insults [25,26]. Thus, as a control group, mice with injuries to the lateral cortex (Lateral group) were prepared in addition to Naive group (Fig. 3A).

At 4 DPI, some DCX(+) cells with a morphology of radial migration were detected around the SVZ in the Medial and Lateral groups (data not shown). GFAP(+) astrocytes and Iba1(+) microglia in the medial striatum had activated morphologies: upregulation of immunoreactivity, large cell bodies, and thick processes (Fig. 3B and 3C). A small number of process-extending DCX(+) cells was detected around the injured cortices of mice in the injured groups (Fig. 3D and 3E, arrows).

At 17 DPI, activation of astrocytes and microglia had almost ceased in the striatum of mice in the Medial and Lateral groups (Fig, 4). At this stage, we analyzed the proliferation and migration of neural stem/precursor cells. First, the numbers of Ki67(+) proliferating cells in the SVZ were not significantly different among the three experimental groups (Fig. 5A and 5B). Second, cell migration from the SVZ/RMS to the OB was analyzed. Seven days prior to mice being euthanized, BrdU was injected to label proliferating cells in the SVZ/RMS. During the remaining period the mice were alive, BrdU-labeled cells reached the OB (Fig. 5C and 5D)[27]. The numbers of BrdU(+) cells in the core of the OB (an extension of the RMS, area 1, Fig. 5E) and in the granule cell layer (area 2, Fig. 5F) were not significantly different. Outside of the SVZ–RMS–OB system, there was a small number of BrdU(+) cells in the striatum far from the SVZ in all experimental groups. Virtually all of these BrdU(+) cells were Olig2(+) oligodendrocytes/oligodendrocyte precursors, but they were not neuronal cells, in any of the experimental groups (Supplemental Fig 4).

Finally, DCX(+) migrating neuroblasts around the SVZ were qualitatively and quantitatively analyzed. Cells with a morphology migrating toward to the injury site were not identified in either the Medial or Lateral groups (data not shown). In all experimental groups, most DCX(+) cells were localized in the SVZ, but a small number of DCX(+) cells was present around all sides of the SVZ, with short distances (Fig. 6A). These DCX(+) cells formed clusters (Fig. 6A and 6B, arrows). In the coronal sections, no processes of DCX(+) cells in the striatum close to the SVZ could be identified in any of the experimental conditions (Fig. 6B). The number (Fig. 6C) and size (number of cells in each cluster, Fig. 6D) of clusters were significantly larger in the Medial group compared with the other experimental groups.

4. Discussion

It had been unclear whether glutamate from the cerebral cortex affect adult neurogenesis in the SVZ. In this study, we analyzed this issue *in vivo*.

First, we examined cortical projection to the SVZ. The medial cortex bilaterally projects axons to the medial striatum close to the SVZ and the lateral septum [18–20,23]. Moreover, cortical axons from the medial cortex invade the striatum from the dorsolateral area of the SVZ, where abundant neural precursors are present [28]. Our results supported these reports, and we detected DsRed-labeled

cortical axons on all areas of the SVZ; these axons were in contact with DCX(+) cells. During development, neurons extend processes widely in their immature stages, but excessive processes are pruned and final connections are established during maturation [29]. Moreover, the maturation of the SVZ occurs during the postnatal stages [30]. Based on our data, we hypothesized that axons from the medial cortex have some effect on the postnatal maturation of the SVZ and neurogenesis in adults.

To test our hypothesis, injuries were made to the bilateral medial cortex. We detected the activation of neurogenesis and DCX(+) cells with a morphology of radial migration that grew toward the injured sites in both the Medial and Lateral groups, at 4 DPI. These phenomena are likely the result of the injury itself, because activation of glial cells was also detected [25,26].

On the other hand, at 17 DPI, the activation of microglia and astrocytes ceased in the injured groups. At this stage, cell proliferation in the SVZ and tangential cell migration to the OB were not significantly different between any of the experimental groups. A small number of DCX(+) cell clusters was detected in the striatum close to the SVZ. The number and size of DCX(+) cell clusters in the Medial group was the largest among all of the experimental groups. DCX(+) leading processes in the clusters were not detected in the coronal sections, while a small number of BrdU(+) glial cells was detected in the striatum far from the SVZ. Even in the Naive mice, there was a small number of proliferating oligodendrocyte precursors in the brain parenchyma [31]. Thus, clusters of Type A cells outside the SVZ should tangentially migrate to the OB. These results suggest that cortical input might inhibit the radial migration of Type A cells. In fact, during the early postnatal stages (around P7), newly generated neuroblasts spread out from the germinal area around the LVs to widespread forebrain regions, with widespread postnatal neurogenesis ceasing afterward [32–34]. This time course matches with the development of axonal projection from the medial cortex as described in the present study. Thus, our results suggest that the cortical glutamatergic input converges with the migration pathway of Type A cells. The activation of GluK5 might be involved in this phenomenon. At present, GluK5 is the sole glutamatergic receptor known to have an inhibitory effect on the migration of Type A cells [14].

5. Conclusion

Axons from the medial cortex came into contact with Type A cells in the postnatal mouse SVZ. The cortical input to Type A cells should converge with their migration pathway in the SVZ/RMS.

Date availability

Data will be available from the corresponding author on request.

Acknowledgments

This research was partly performed at the Tottori Bio Frontier, managed by the Tottori prefecture.

References

[1] K. Obernier, A. Alvarez-Buylla, Neural stem cells: Origin, heterogeneity and regulation in the adult mammalian brain, Dev. 146 (2019).

[2] S.Z. Young, M.M. Taylor, A. Bordey, Neurotransmitters couple brain activity to subventricular zone neurogenesis., Eur J Neurosci. 33 (2011) 1123–1132.

[3] G.U. Höglinger, P. Rizk, M.P. Muriel, C. Duyckaerts, W.H. Oertel, I. Caille, E.C. Hirsch, Dopamine depletion impairs precursor cell proliferation in Parkinson disease., Nat Neurosci. 7 (2004) 726–35.

[4] J.M. Brezun, A. Daszuta, Depletion in serotonin decreases neurogenesis in the dentate gyrus and the subventricular zone of adult rats, Neuroscience. 89 (1999) 999–1002.

[5] M. Banasr, M. Hery, R. Printemps, A. Daszuta, Serotonin-induced increases in adult cell proliferation and neurogenesis are mediated through different and common 5-HT receptor subtypes in the dentate gyrus and the subventricular zone., Neuropsychopharmacology. 29 (2004) 450–60.

[6] C.K. Tong, J. Chen, A. Cebrián-Silla, Z. Mirzadeh, K. Obernier, C.D. Guinto, L.H. Tecott, J.M. García-Verdugo, A. Kriegstein, A. Alvarez-Buylla, Axonal control of the adult neural stem cell niche., Cell Stem Cell. 14 (2014) 500–11.

[7] S.Z. Young, M.M. Taylor, S. Wu, Y. Ikeda-matsuo, C. Kubera, A. Bordey, NKCC1 knockdown decreases neuron production through GABA(A)-regulated neural progenitor proliferation and delays dendrite development., J Neurosci. 32 (2012) 13630–8.

[8] X. Liu, Q. Wang, T.F. Haydar, A. Bordey, Nonsynaptic GABA signaling in postnatal subventricular zone controls proliferation of GFAP-expressing progenitors., Nat Neurosci. 8 (2005) 1179–1187.

[9] A.J. Bolteus, A. Bordey, GABA release and uptake regulate neuronal precursor migration in the postnatal subventricular zone., J Neurosci. 24 (2004) 7623–7631.

[10] S.Z. Young, C.A. Lafourcade, J.-C. Platel, T. V. Lin, A. Bordey, GABAergic striatal neurons project dendrites and axons into the postnatal subventricular zone leading to calcium activity., Front Cell Neurosci. 8 (2014) 10.

[11] J.N.C. Kew, J.A. Kemp, Ionotropic and metabotropic glutamate receptor structure and pharmacology., Psychopharmacology (Berl). 179 (2005) 4–29.

[12] M. Götz, S. Sirko, J. Beckers, M. Irmler, Reactive astrocytes as neural stem or progenitor cells: In vivo lineage, In vitro potential, and Genome-wide expression analysis., Glia. 63 (2015) 1452–68.

[13] V. Di Giorgi-Gerevini, D. Melchiorri, G. Battaglia, L. Ricci-Vitiani, C. Ciceroni, C.L. Busceti, F. Biagioni, L. Iacovelli, a M. Canudas, E. Parati, R. De Maria, F. Nicoletti, Endogenous activation of metabotropic glutamate receptors supports the proliferation and

survival of neural progenitor cells., Cell Death Differ. 12 (2005) 1124–33.

[14] J.-C. Platel, T. Heintz, S. Young, V. Gordon, A. Bordey, Tonic activation of GLUK5 kainate receptors decreases neuroblast migration in whole-mounts of the subventricular zone., J Physiol. 586 (2008) 3783–3793.

[15] J.-C. Platel, K.A. Dave, V. Gordon, B. Lacar, M.E. Rubio, A. Bordey, NMDA receptors activated by subventricular zone astrocytic glutamate are critical for neuroblast survival prior to entering a synaptic network., Neuron. 65 (2010) 859–72.

[16] M. Song, S.P. Yu, O. Mohamad, W. Cao, Z.Z. Wei, X. Gu, M.Q. Jiang, L. Wei, Optogenetic stimulation of glutamatergic neuronal activity in the striatum enhances neurogenesis in the subventricular zone of normal and stroke mice, Neurobiol Dis. 98 (2017) 9–24.

[17] Z. Zhang, X. Zheng, Y. Liu, Y. Luan, L. Wang, L. Zhao, J. Zhang, Y. Tian, H. Lu, X. Chen, Y. Liu, Activation of metabotropic glutamate receptor 4 regulates proliferation and neural differentiation in neural stem/progenitor cells of the rat subventricular zone and increases phosphatase and tensin homolog protein expression., J Neurochem. 156 (2021) 465–480.

[18] B.J. Hunnicutt, B.C. Jongbloets, W.T. Birdsong, K.J. Gertz, H. Zhong, T. Mao, A comprehensive excitatory input map of the striatum reveals novel functional organization., Elife. 5 (2016) 1–32.

[19] S.R. Sesack, A.Y. Deutch, R.H. Roth, B.S. Bunney, Topographical organization of the efferent projections of the medial prefrontal cortex in the rat: an anterograde tract-tracing study with Phaseolus vulgaris leucoagglutinin., J Comp Neurol. 290 (1989) 213–42.

[20] C. Fillinger, I. Yalcin, M. Barrot, P. Veinante, Efferents of anterior cingulate areas 24a and 24b and midcingulate areas 24a' and 24b' in the mouse., Brain Struct Funct. 223 (2018) 1747–1778.

[21] T. Saito, In vivo electroporation in the embryonic mouse central nervous system., Nat Protoc. 1 (2006) 1552–8.

[22] Y. Kanda, Investigation of the freely available easy-to-use software 'EZR' for medical statistics, Bone Marrow Transplant. 48 (2013) 452–458.

[23] U.S. Sohur, H.K. Padmanabhan, I.S. Kotchetkov, J.R.L. Menezes, J.D. Macklis, Anatomic and molecular development of corticostriatal projection neurons in mice., Cereb Cortex. 24 (2014) 293–303.

[24] B.J. Molyneaux, P. Arlotta, J.R.L. Menezes, J.D. Macklis, Neuronal subtype specification in the cerebral cortex., Nat Rev Neurosci. 8 (2007) 427–37.

[25] E.H. Chang, I. Adorjan, M. V. Mundim, B. Sun, M.L. V Dizon, F.G. Szele, Traumatic Brain Injury Activation of the Adult Subventricular Zone Neurogenic Niche., Front Neurosci. 10 (2016) 332.

[26] M. Ceanga, M. Dahab, O.W. Witte, S. Keiner, Adult Neurogenesis and Stroke: A Tale of Two Neurogenic Niches., Front Neurosci. 15 (2021) 700297.

[27] C. Lois, A. Alvarez-Buylla, Long-Distance Neuronal Migration in the Adult Mammalian

Brain, Science (80-). 264 (1994) 1145–1148.
[28] W. Shi, M. Xue, F. Wu, K. Fan, Q.-Y. Chen, F. Xu, X.-H. Li, G.-Q. Bi, J.-S. Lu, M. Zhuo, Whole-brain mapping of efferent projections of the anterior cingulate cortex in adult male mice., Mol Pain. 18 (2022) 17448069221094528.
[29] G.M. Innocenti, D.J. Price, Exuberance in the development of cortical networks, Nat Rev Neurosci. 6 (2005) 955–965.
[30] A.D. Tramontin, J.M. García-Verdugo, D. a Lim, A. Alvarez-Buylla, Postnatal development of radial glia and the ventricular zone (VZ): a continuum of the neural stem cell compartment., Cereb Cortex. 13 (2003) 580–7.
[31] T. Mori, T. Wakabayashi, Y. Takamori, K. Kitaya, H. Yamada, Phenotype Analysis and Quantification of Proliferating Cells in the Cortical Gray Matter of the Adult Rat, Acta Histochem Cytochem. 42 (2009) 1–8.
[32] J. Wright, D. Stanic, L.H. Thompson, Generation of striatal projection neurons extends into the neonatal period in the rat brain., J Physiol. 591 (2013) 67–76.
[33] S.D.E. Marchis, A. Fasolo, A.C. Puche, S. De Marchis, A. Fasolo, A.C. Puche, S.D.E. Marchis, A. Fasolo, A.C. Puche, S. De Marchis, A. Fasolo, A.C. Puche, Subventricular zone-derived neuronal progenitors migrate into the subcortical forebrain of postnatal mice., J Comp Neurol. 476 (2004) 290–300.
[34] D. Inta, J. Alfonso, J. von Engelhardt, M.M. Kreuzberg, A.H. Meyer, J. a van Hooft, H. Monyer, Neurogenesis and widespread forebrain migration of distinct GABAergic neurons from the postnatal subventricular zone., Proc Natl Acad Sci U S A. 105 (2008) 20994–20999.

Figure legends

Figure 1
DsRed-labeled axons from the medial cortex and their contacts with DCX(+) cells. Dorsolateral (A), septal (B), and striatal (C) areas of the SVZ are shown. Arrows indicate varicosities contacting with DCX(+) cells. Dashed lines indicate the borders of the SVZ. Stacked confocal microscopy images are shown. (C') High magnification-single optical confocal microscopy images of the boxed area in C. A varicosity of a DsRed(+) axon contacted with a DCX(+) cell (arrow). Str, striatum; Sep, septum; LV, lateral ventricle. Scale bar = 20 μm for A-C and 5 μm for C'.

Figure 2
Maturation of the corticostriatal projection and the SVZ during the postnatal stages. The corticostriatal axons were diffusely distributed in the striatum at P7 (A-C), but they localized to the medial striatum up until P21 (D-F). High-magnification images of the SVZ are shown in the boxed areas, stained with

Hoechst 33258 (A’ and D’). The GFAP-immunostaining pattern matured during the postnatal stages. At P7, some GFAP(+) cells radially extended processes from the SVZ to the lateral striatum (B, C). At P21, GFAP(+) radial processes localized around the SVZ (E, F). Epifluorescence microscopy images of the ipsilateral striatum are shown. The asterisks indicate injection sites where plasmid was introduced. Scale bars = 500 μm in A; 50 μm in A' for A’ and D’;500 μm in D; 50 μm in B for B, C, E, and F.

Figure 3

Effects of bilateral injury to the cortex at 4 days post-injury (DPI). The images show hematoxylin and eosin (HE) staining of bilateral cortical stab injuries (A). At 4 DPI, GFAP(+) astrocytes (B) and Iba1(+) microglia (C) in the medial striatum had a morphology of activation in the Medial and Lateral groups. (D and E) Around the injury sites, DCX(+) young neurons with a process were detected in the Medial and Lateral groups (arrows), but not in the Naive group (data not shown). Stacked confocal microscopy images (B, C, and lower panels in D and E) and epifluorescence microscopy images (D and E upper panels) are shown. Scale bars = 500 μm in A; 20 μm in B for B and C; 100 μm (upper panel) and 10 μm (lower panel) in D for D and E.

Figure 4

Effects of bilateral injury to the cortex at 17 DPI. By 17 DPI, activation of astrocytes (A) and microglia (B) had almost ceased in the Medial and Lateral groups. Stacked confocal microscopy images are shown. (C) Signal intensities of Iba1 immunostaining at 17 DPI. The mean fluorescence intensities in the medial halves of the striatum were analyzed. There was no significant difference between all experimental conditions. n = 5 mice in each condition. The Kruskal–Wallis test was performed. Scale bar = 20 μm in A for A and B.

Figure 5

Cortical injury had no significant effect on cell proliferation in the SVZ or tangential migration to the olfactory bulb (OB). Epifluorescence microscopy images of Ki67(+) proliferating cells (A) and quantification of Ki67(+) cells (B) in the SVZ. High-magnification images are shown in the boxed areas. Epifluorescence microscopy images of BrdU(+) cells that had migrated to the OB (C and D) and quantification of BrdU(+) cells in area 1 (an extension of the RMS, E) and area 2 (the granule cell layer, F). There was no significant difference in the numbers of Ki67(+) cells and BrdU(+) cells among any of the experimental conditions (B, E, and F). One-way ANOVA (B and F) or the Kruskal–Wallis test (E) was performed. Four (B, Ki67) or three (E and F, BrdU) sections per mouse were analyzed. n = 6 mice in each group. N.S., not significant. Scale bars = 300 μm and 100 μm in A for low- and high-magnification images, respectively; 100 μm in C; 200 μm in D.

Figure 6

DCX(+) cell clusters in the striatum close to the SVZ. There was a small number of DCX(+) cell clusters in the striatum close to the SVZ in all experimental conditions, but there were more DCX(+) clusters in the Medial group (A). Arrows indicate DCX(+) cell clusters. High-magnification images are shown in the boxed areas. Epifluorescence microscopy images are shown. (B) Stacked confocal microscopy images of DCX(+) cells in a cluster. Leading processes were not detected in the coronal sections. The number (C) and size (D) of DCX(+) cell clusters were the largest in the Medial group among all experimental conditions. One-way ANOVA followed by Tukey's *post hoc* test (C) or the Kruskal–Wallis test followed by the Steel–Dwass test (D) were performed. Four sections per mouse were analyzed. $n = 6$ mice in each condition. * $p < 0.05$, ** $p < 0.01$. Scale bars = 200 μm and 50 μm in A for low- and high-magnification images, respectively; 10 μm in B.

Supplemental Figure 1

Introduction of DsRed-expressing plasmid vector to the medial cortex. *In utero* electroporation was performed at E14 and the embryos were fixed at E16. Epifluorescence microscopy images are shown. LGE, lateral ganglionic eminence. Scale bars = 300 μm, 200 μm, and 300 μm in A, A1 and A2, respectively.

Supplemental Figure 2

Axonal projection from the medial cortex to the striatum at P21. The asterisk indicates the cingulate cortex where DsRed-expressing plasmid vector was introduced at E14. The cingulate cortex projected axons to the lateral septum (A1), contralateral cingulate cortex, ipsilateral (A2 and A4) and contralateral (A3 and A5) medial striatum,. Epifluorescence microscopy images are shown. Scale bars = 500 μm, 50 μm, 300 μm, and 50 μm in A, A1, A3, and A5 respectively.

Supplemental Figure 3

A synapsin 1(+)/DsRed(+) varicosity contacting with a DCX(+) cell in the striatal SVZ at P21. An anti-synapsin 1 antibody, a marker of synapses, labeled the varicosities that were in contact with DCX(+) cells. Single optical confocal microscopy images (single) and a stacked confocal microscopy image (stacked) are shown. Scale bar = 5 μm.

Supplemental Figure 4

Identification of BrdU(+) cells in the striatum far from the SVZ at 17 DPI. Single optical confocal microscopy images of Naive (A, C, and E) and Medial groups (B, D, and F) are shown. There was a small number of BrdU(+) cells in the striatum far from the SVZ. Virtually all BrdU(+) cells were Olig2(+) oligodendrocyte lineage cells (A and B), but neither DCX(+) immature neurons(C and D) nor NeuN(+) mature neurons (E and F). Scale bar = 10 μm.

Table 1 Primary and secondary antibodies

Antigen and conjugation	Raised in	Provider, product ID	RRID	Dilution
BrdU	rat	Abcam, #ab6326	AB_305426	1:200
Doublecortin (DCX)	goat	Santa Cruz, #sc8066	AB_2088494	1:100
Doublecortin (DCX)	guinea pig	Chemicon, #AB2253	AB_1586992	1:2,000
Glial fibrillary acidic protein (GFAP)	rabbit	DAKO, #Z0334	AB_10013382	1:1,000
Iba1	rabbit	Wako, #019-19741	AB_839504	1:1,000
Ki67	rabbit	Novocastra, #NCL-Ki67p	AB_442102	1:2,000
NeuN	rabbit	Abcam, #ab177487	AB_2532109	1:10,000
Olig2	goat	Santa Cruz, #sc19969	AB_2236477	1:400
Red fluorescent protein (RFP)	rabbit	MBL, #PM005	AB_591279	1:5,000
Red fluorescent protein (RFP)	goat	Rockland, #200-101-379	AB_2744552	1:1,000

Red fluorescent protein (RFP)	guinea pig	Frontier Institute, #MSFR101410	AB_2571648	1:400
Synapsin 1	rabbit	CST, #5297	AB_2616578	1:1,000
Rabbit IgG, AlexaFluor 488 conjugated	donkey	Invitrogen, #A21206	AB_2535792	1:800
Rabbit IgG, AlexaFluor 555 conjugated	donkey	Invitrogen, #A31572	AB_162543	1:800
Rat IgG, AlexaFluor 488 conjugated	donkey	Invitrogen, #A21208	AB_2535794	1:800
Rat IgG, Cy3 conjugated	donkey	Jackson, #712-165-153	AB_2340667	1:200
Goat IgG, Cy3 conjugated	donkey	Jackson, #705-165-147	AB_2307351	1:200
Goat IgG, Cy5 conjugated	donkey	Jackson, #705-175-147	AB_2340415	1:200
Guinea pig IgG, Cy2 conjugated	donkey	Jackson, #706-225-148	AB_2340467	1:200
Guinea pig IgG, Cy3 conjugated	donkey	Jackson, #706-165-148	AB_2340460	1:200

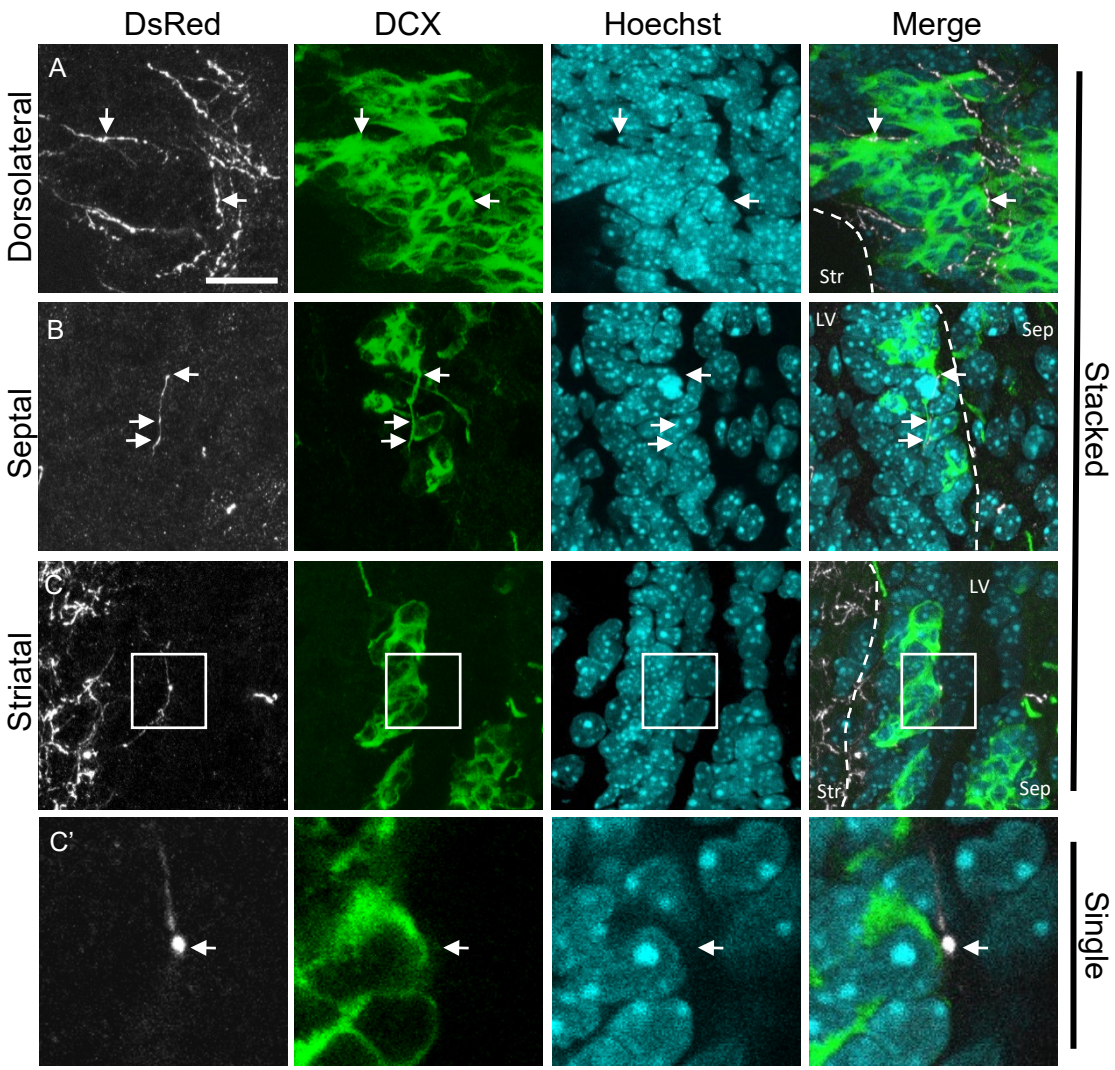
DsRed
DCX
Hoechst
Merge
A
B
C
C'
Dorsolateral
Septal
Striatal
Str
LV
Sep
Stacked
Single

Figure 1

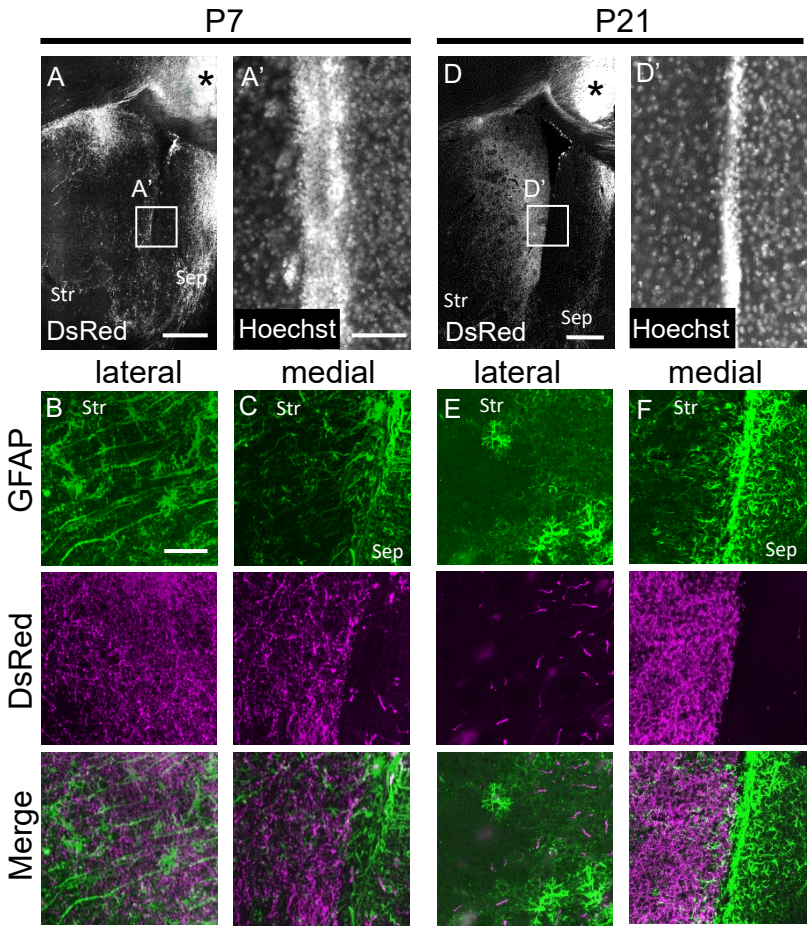
P7
P21
A
A'
D
D'
*
*
A'
D'
Str
Sep
DsRed
Hoechst
lateral
medial
lateral
medial
B
C
E
F
GFAP
DsRed
Merge

Figure 2

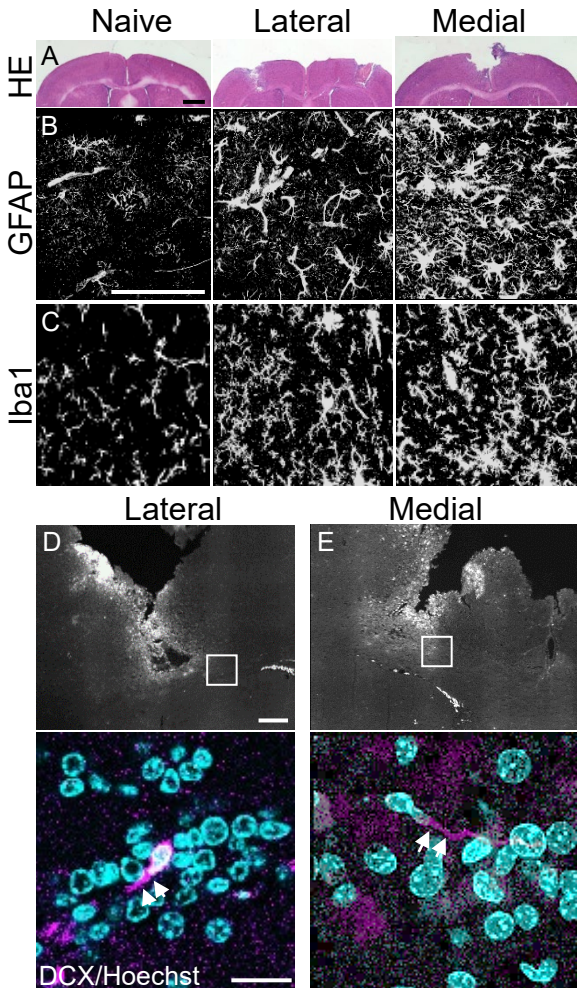
Naive
Lateral
Medial
HE
A
GFAP
B
Iba1
C
Lateral
Medial
D
E
DCX/Hoechst

Figure 3

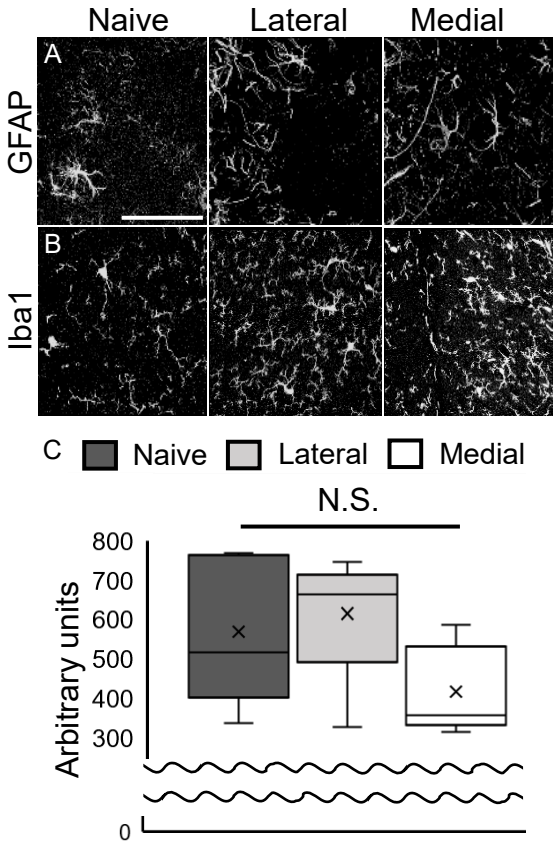
Naive
Lateral
Medial
A
GFAP
B
Iba1
C
Naive
Lateral
Medial
N.S.
800
700
600
500
400
300
Arbitrary units
0

Figure 4

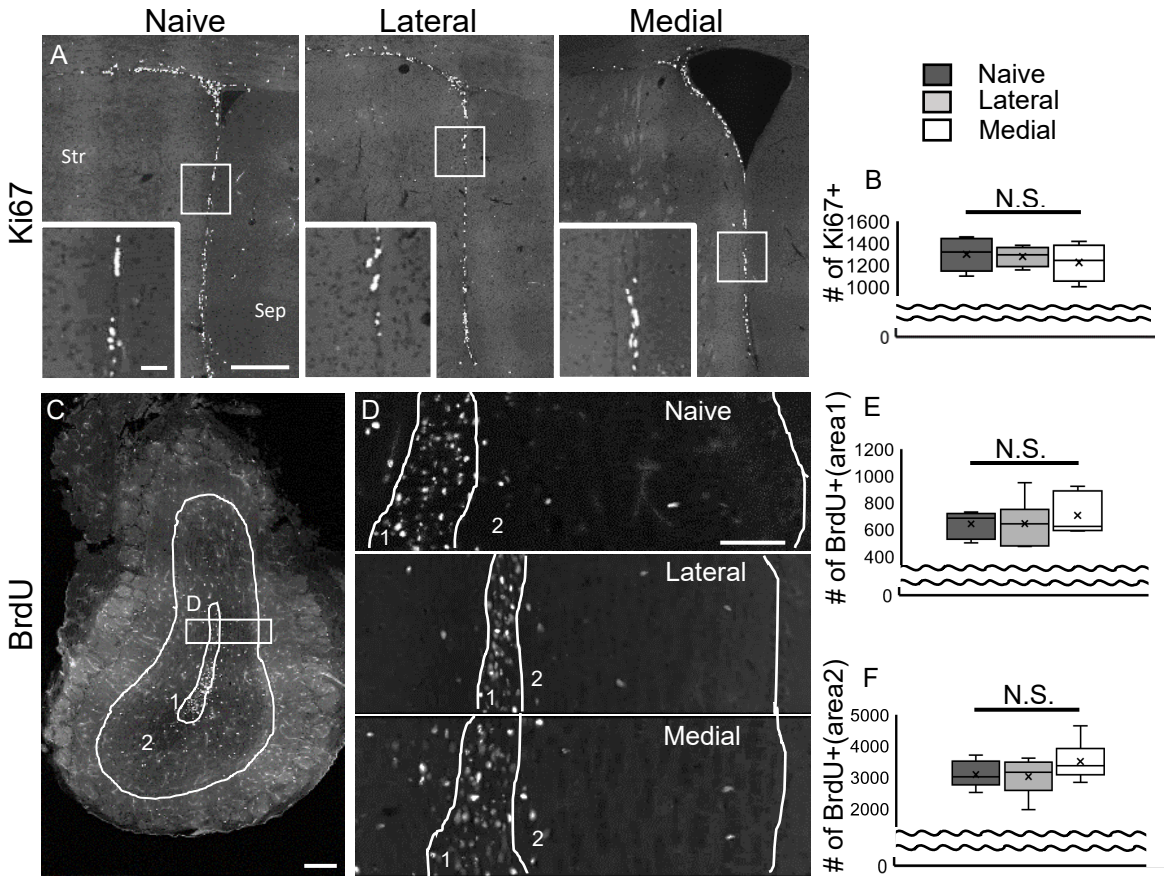
Naive
Lateral
Medial
Ki67
BrdU
A
Str
Sep
B
N.S.
# of Ki67+
1600
1400
1200
1000
0
C
D
1
2
D
Naive
Lateral
Medial
E
N.S.
# of BrdU+(area1)
1200
1000
800
600
400
0
F
N.S.
# of BrdU+(area2)
5000
4000
3000
2000
0

Figure 5

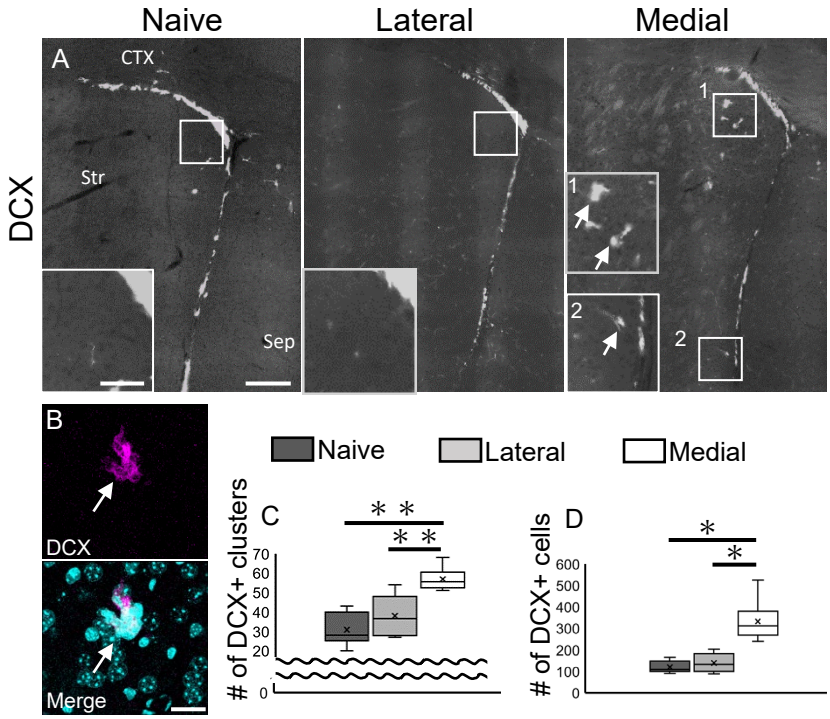
Naive
Lateral
Medial
A
CTX
Str
Sep
DCX
1
2
B
DCX
Merge
Naive
Lateral
Medial
C
# of DCX+ clusters
70
60
50
40
30
20
0
D
# of DCX+ cells
600
500
400
300
200
100
0

Figure 6

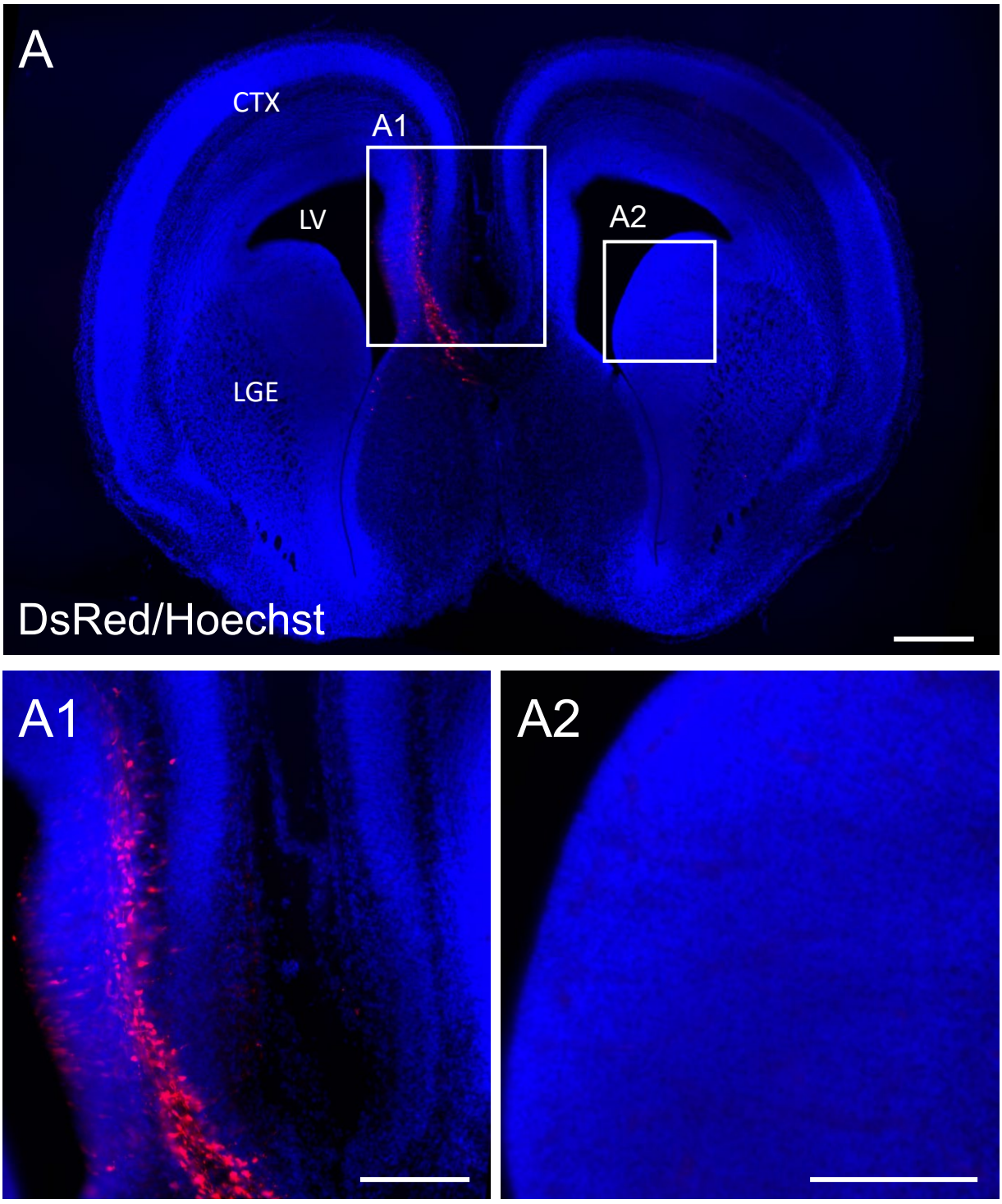

Supplemental Figure 1

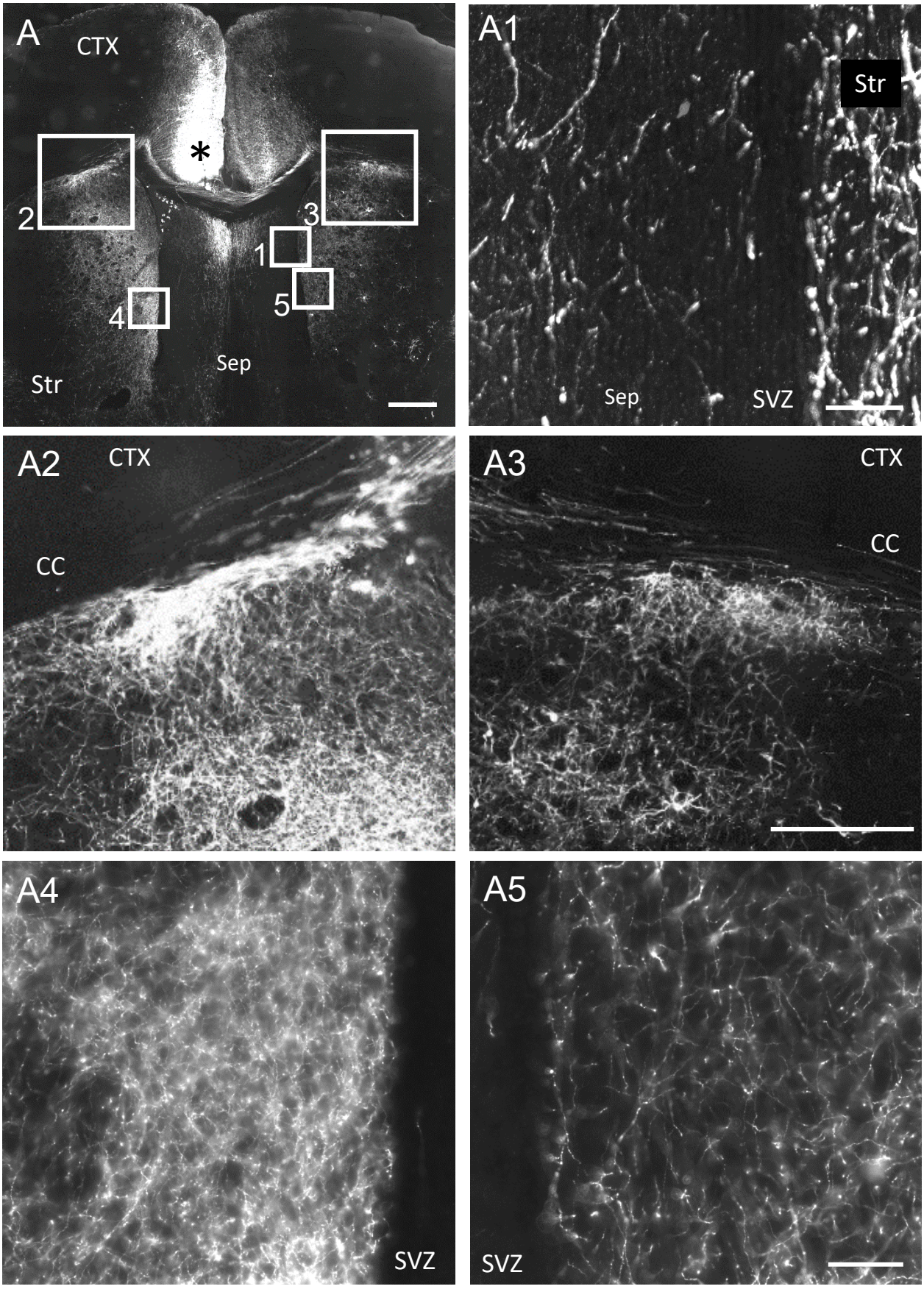

Supplemental Figure 2

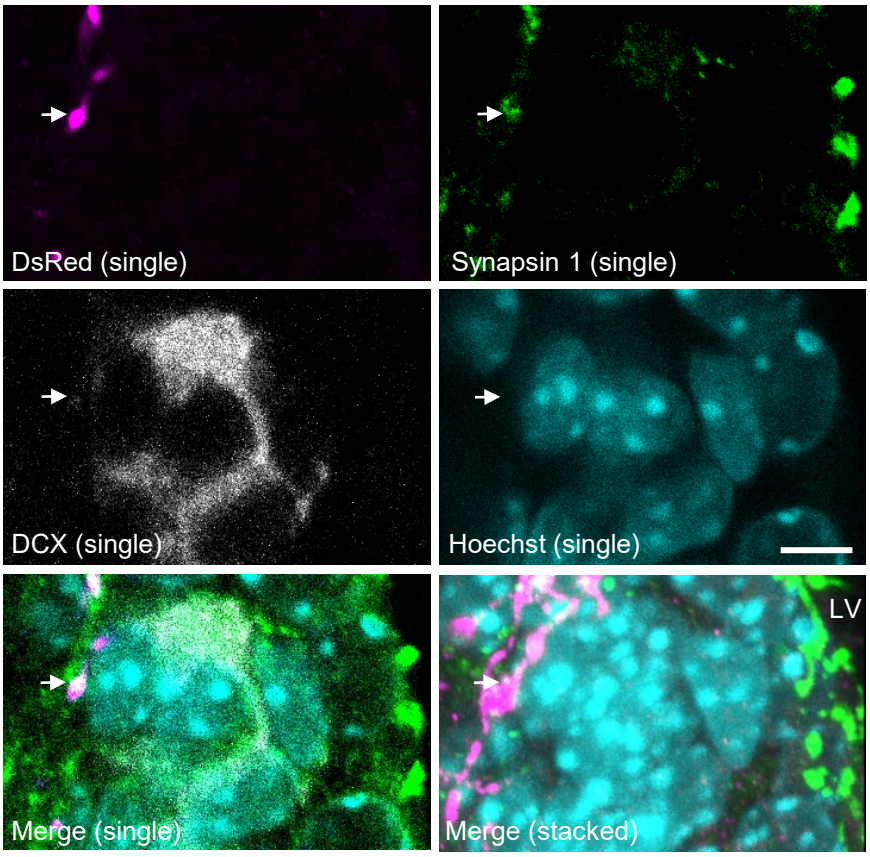

Supplemental Figure 3

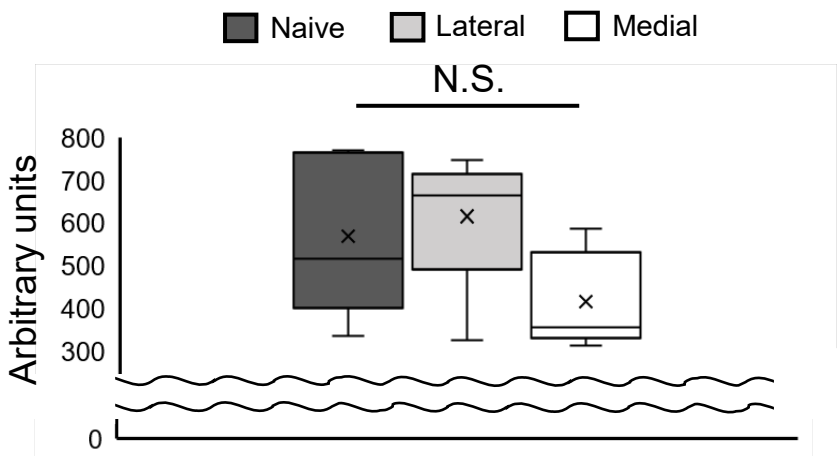

Supplemental Figure 4

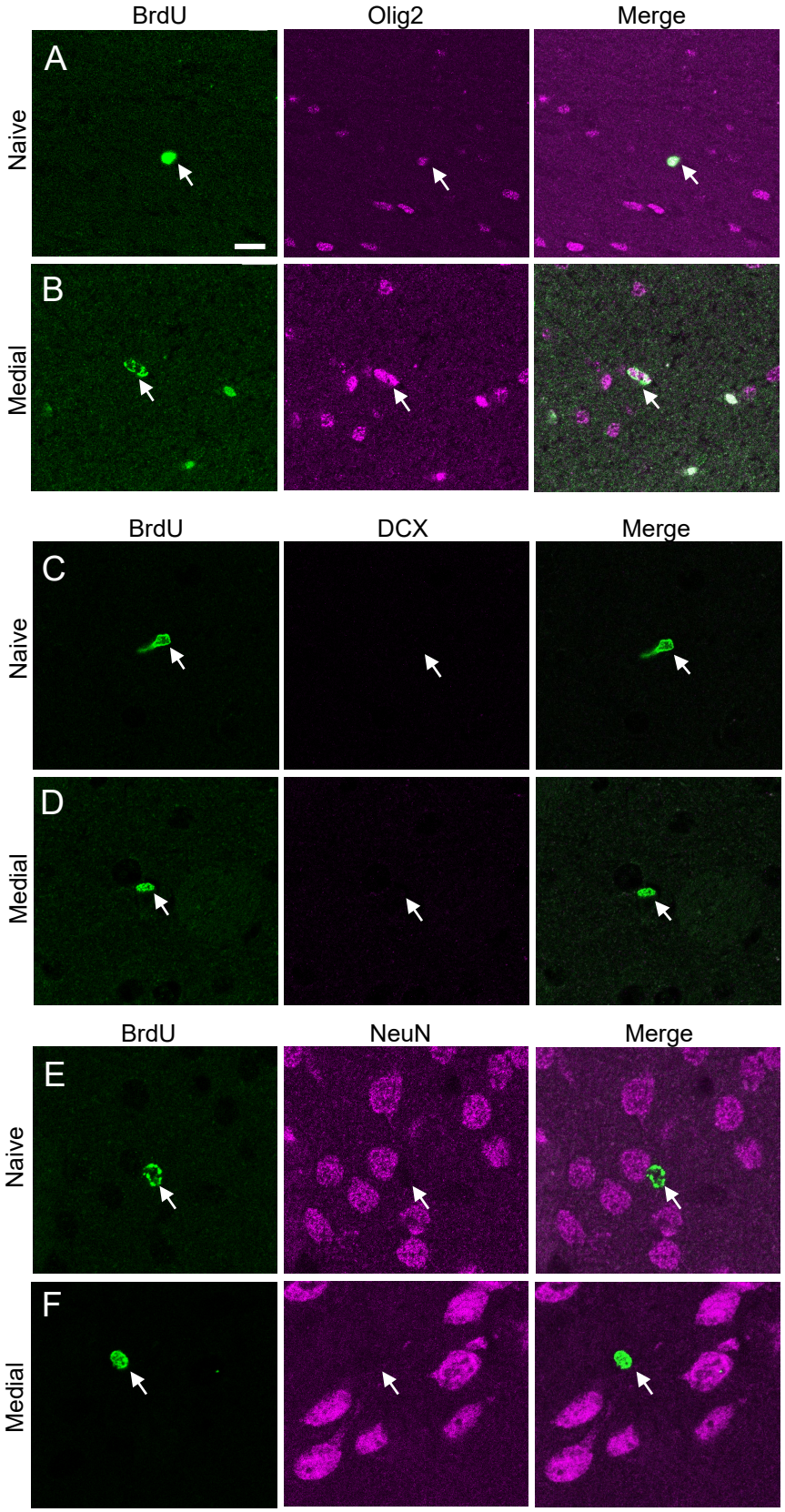

Supplemental Figure 5